Computational and theoretical analysis of weak and strong transverse-wave structures in gaseous detonations

Ralf Deiterding[1]

[1]Oak Ridge National Laboratory, P.O. Box 2008 MS6367, Oak Ridge, TN 37831

E-mail: deiterdingr@ornl.gov

Abstract. Two-dimensional simulation results are presented that capture at great detail the temporal evolution of Mach reflection triple point sub-structures intrinsic to gaseous detonation waves. The observed patterns are classified by shock polar analysis for realistic, thermally perfect but nonreactive gases. A diagram of the transition boundaries between possible Mach reflection structures is constructed and found to be in good agreement with the computational results.

1. Introduction

The propagation of detonation waves in gaseous media is characterized by the appearance of transverse pressure waves propagating perpendicular to the detonation front. The hydrodynamic flow pattern around the resulting triple points is a Mach reflection phenomenon under transient conditions. Although the problem has received considerable attention (cf. [9]), no comprehensive theory is available yet to accurately predict the detailed multi-dimensional flow behavior.

In the present paper, we use high-resolution numerical simulation to analyze the hydrodynamic details of two-dimensional Chapman-Jouguet (CJ) detonations in low-pressure hydrogen-oxygen with high argon dilution. In free space, the triple point movement in such mixtures is very regular leading to a repetitive triple point trajectory pattern of regular "detonation cells" [8]. We study a series of computations in which the regularly oscillating detonation propagates through a smooth pipe bend of varying angle. It is found that nonreactive shock wave reflection theory [1], extended for thermally perfect gas mixtures, is applicable to classify the observed transient triple point structures as transitional and double Mach reflection patterns.

2. Computational Method

The used simulation code solves the Euler equations for multiple thermally perfect species with chemically reactive source terms. All species are assumed to be thermally perfect gases with temperature dependent enthalpy $h_i\,(T) = h_i^0 + \int_{To}^{T} c_{pi}\,(\sigma)\,d\sigma$ [6]. The chemical production rates are modeled with a hydrogen-oxygen reaction mechanism of 34 elementary reactions that considers the species H, O, OH, H_2, O_2, H_2O, HO_2, H_2O_2 and Ar [10].

A time-operator splitting approach is adopted to decouple hydrodynamic transport and chemical reaction numerically. A semi-implicit Rosenbrock-Wanner method is used to integrate the kinetics, and a shock-capturing finite volume discretization is employed to achieve proper upwinding in all characteristic fields. The finite volume scheme utilizes a quasi-one-dimensional approximate Riemann solver of Roe-type and is extended to multiple space dimensions via the method of fractional steps.

Special corrections are applied to avoid unphysical total densities and internal energies, to ensure positive mass fractions, and to prevent the carbuncle phenomenon. The MUSCL-Hancock variable extrapolation technique is adopted to construct a second-order method (see [5] for details).

Geometrically complex moving boundaries are incorporated into the originally Cartesian upwind method by utilizing some of the finite volume cells as ghost cells to enforce immersed rigid wall boundary conditions [5]. Slight approximation errors due to this approach are alleviated by dynamic mesh adaptation.

Since the accurate numerical simulation of detonation waves mandates a particularly high temporal and spatial resolution near the detonation front, we utilize the structured adaptive mesh refinement (SAMR) algorithm after Berger and Colella [2]. We have implemented the SAMR algorithm in a generic, dimension-independent object-oriented framework in C++ called AMROC. AMROC follows a rigorous domain decomposition approach, suitable for MPI-based distributed memory parallelization, and partitions the SAMR hierarchy from the root level on [3]. The software system has been verified extensively for shock and detonation wave simulation [4]. The latest version exhibits good parallel scalability on $O(1000)$ cores.

3. Results

We study two-dimensional, self-sustained CJ detonations in a $H_2 : O_2 :$ Ar mixture of molar ratios 2 : 1 : 7 at initial temperature 298K and pressure 10.0 kPa. The one-dimensional detonation theory after Zel'dovich, von Neumann, and Döring (ZND) predicts a detonation velocity of 1638.5 m/s, a von Neumann Pressure of ~270 kPa, and a reaction length of 0.878 mm for this mixture. All shown computations use four additional levels of Cartesian mesh adaptation with refinement factors 2, 2, 2, and 4 giving an effective resolution of 67.6 cells within the half reaction length, the distance between shock and reaction zone according to ZND theory. Mesh adaptation is based on a physically motivated combination of scaled gradients of total density and pressure and error estimation by Richardson extrapolation of the mass fractions (cf. [5]).

3.1. Regular Cellular Detonation Structure

The results shown in Figure 1 use as computational domain a square channel of the physical dimensions 1.0 m × 3.2 cm, in which four transverse pressure waves and thereby two perfectly regular detonation cells occur. The base mesh has 2000 × 128 cells. The left graphic of Figure 1 displays triple point trajectories in a part of the computational domain with the detonation front at two time steps overlaid. The trajectories are visualized by tracking the maximum of the magnitude of the vorticity on a uniform auxiliary grid with the mesh widths of the first refinement level. The right graphic of Figure 1 shows the different level of adaptation, indicated by gray scales, for the first time step.

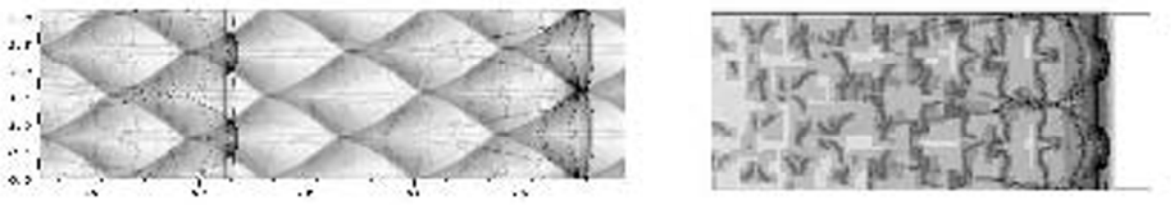

Figure 1. Left: oscillating detonation front on computed triple points tracks in a rectangular channel. Right: schlieren plot of density on refinement levels.

Figure 2 zooms into the situation shortly before the collision of two triple points. The middle enlargement shows clearly that the shock wave pattern around each triple point is of double Mach reflection (DMR) (aka "strong") type. As depicted in the right sketch, the essential flow features around triple point T are: inflow (A), region B behind the Mach stem M, transverse wave region (C),

	p/p_A	ρ/ρ_A	T [K]	v[m/s]	M
A	1.00	1.00	298	1775	5.078
B	31.45	4.17	2248	447	0.477
C	31.69	5.32	1775	965	1.153
D	19.17	3.84	1487	1178	1.533
E	35.61	5.72	1856	901	1.053
F	40.61	6.09	1987	777	0.880

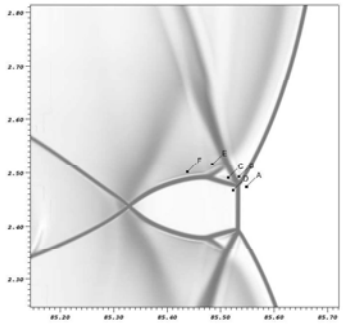

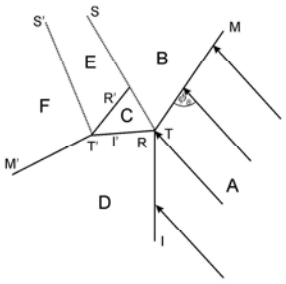

Figure 2. States of a DMR structure shortly before the next collision.

and region D downstream of the incident shock I. Regions B and C are separated by the slip line S, a contact discontinuity. Regions C and D are separated by the reflected shock R. Characteristic for the DMR pattern is a high supersonic velocity in region C that leads to the formation of a further shock R' creating a secondary triple point T' on the transverse wave. The very weak slip line S', emanating from T' between regions E and F, can hardly be inferred. Note that the reflected shock R is the incident shock I' for the secondary triple point T'.

3.2. Transformation into the Frame of Reference of a Triple Point

In order to analyze a Mach reflection pattern quantitatively, it is necessary to map the velocity field of the simulation into a frame of reference attached to the triple point. However, the reliable estimation of the triple point speed v_0 from a single computational time step is non-apparent. When evaluating v_0 we take advantage of the fact that the triple point is formed at the tip, where the Mach stem intersects the incident region, and that the oblique shock relations [1] between two points in regions A and B close to the triple point must hold true. We require only the two relations

$$\rho_A v_A \sin(\phi_B) = \rho_B v_B \sin(\phi_B - \theta_B)\,, \quad (1)$$

$$p_A + \rho_A v_A^2 \sin^2(\phi_B) = p_B + \rho_B v_B^2 \sin^2(\phi_B - \theta_B)\,. \quad (2)$$

Inserting Eq. (1) into Eq. (2) allows the elimination of $v_B \sin(\phi_B - \theta_B)$, which yields

$$v_A = \frac{1}{\sin\phi_B}\sqrt{\frac{\rho_B(p_B - p_A)}{\rho_A(\rho_B - \rho_A)}}\,.$$

As the gas is initially at rest, the triple point velocity is $v_0 = -v_a$ and ϕ_B, the angle of inflow, is given as the angle between Mach stem front and the triple point trajectory, which can be measured from visualizations such as the left one of Figure 1. The states close of the triple point of Figure 2 are given in the table of Figure 2. Since the triple point is far ahead of the reaction region, changes in mixture are neglected in evaluating the Mach number M in the triple point pattern. As it can be expected in a DMR [1], M_C is clearly greater than 1.

A further important quantity for triple point structures is the strength S of the transverse wave [7] that is defined as $S := \frac{pC - pD}{pD}$. For the present computation, S is rather constant throughout one regular detonation cell and varies around 0.65.

3.3. Detonation Structure in Smooth Pipe Bends

In order to study triple point structures under transient conditions, we simulate the propagation of the regularly oscillating detonation through smooth pipe bends of varying angles. The computations are initialized by reproducing a single detonation cell of the previous computation five times 13 cm before the beginning of the curved section. For instance, for bend angle $\varphi = 60°$, with a base mesh of 1200 ×

992 cells, the adaptive computation uses approximately 7.1 M to 3.4 M cells on all and 4.8 M to 1.8 M cells on the highest level instead of ~1, 219 M in the uniform case. The calculations were run on 64 Intel Xeon 2.4GHz dual-processor nodes with Quadrics interconnect and required nevertheless ~70,000 h CPU each (~23 days wall time).

The diffraction and compression of the detonation wave at the bend leads to changes of the transverse wave strength *S*. While the state *C* behind the reflected shock *R* remains initially unchanged, the change in geometry alters the incident state *D*. Near the inner bend wall, the incident pressure p_D drops, leading to a considerable increase in *S*. The resulting triple point structure is of strengthened DMR type with larger detonation cells (cf. Right graphic of Figure 3) and increased M_C. In the compression region near the outer wall, however, p_D increases drastically leading to a considerable decrease of *S*. As a consequence, the flow in region *C* decelerates and the secondary shock *R'* between *C* and *E* is no longer necessary for a stable configuration. The triple point now exhibits a transitional Mach reflection (TMR) or "weak" pattern. Characteristic for the TMR structure is that the flow in region *C* is then just barely supersonic with respect to *T* [1]. TMR structures are also found in the diffraction region when a sufficiently large angle φ causes partial detonation failure.

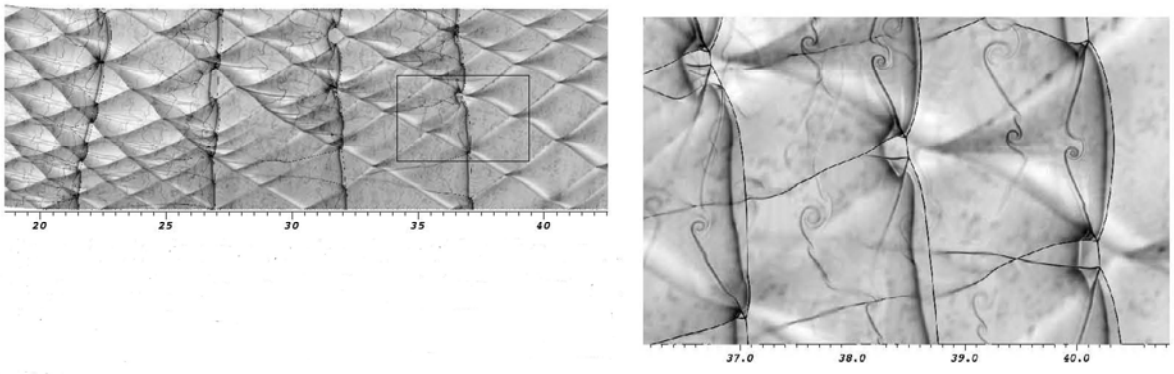

Figure 3. Left: cellular structure after the bend for φ = 15°. Right: triple point re-initiation with change from TMR to DMR. The physical time steps 200 μs, 210 μs, and 220 μs are shown.

The right graphic of Figure 3 depicts the interesting case of triple point re-initiation after the bend for φ = 15°. The new triple point in the center of the graphic is formed as a weak structure (TMR) but strengthens into a DMR after its first collision. Figure 4 visualizes the quenching of triple points at the outer bend wall that occurs for all larger values of φ. As can be inferred from the left graphic of Figure 4, failing triple points with vanishing trajectories seem to exhibit a weak structure.

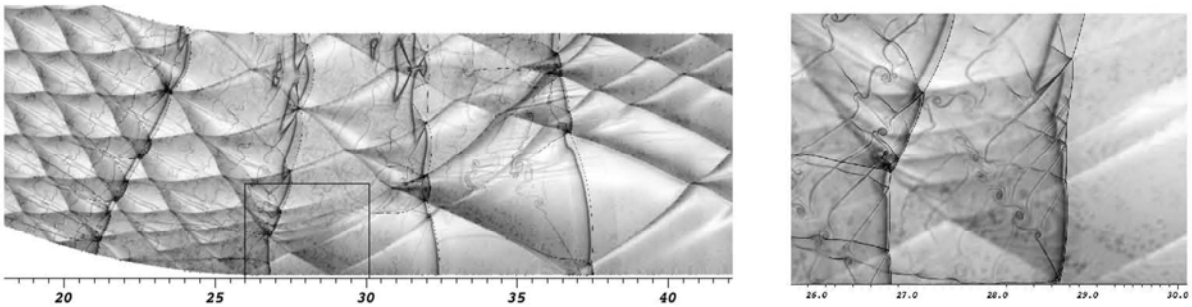

Figure 4. Left: cellular structure immediately after the bend for φ = 30°. Right: triple point quenching and failure as SMR at 140 μs and 150 μs simulated physical time.

3.4. Transition Criteria of Mach Reflection Phenomena

The two dimensional oblique jump conditions [1] are satisfied across each discontinuity depicted in the right sketch of Figure 2. We solve the resulting nonlinear system of equations numerically under the assumption that the composition of the H_2 : O_2 : Ar mixture is invariant, but note that the temperature dependency of the material properties is fully considered. It is well-known (cf. [1]) that changes in Mach reflection type occur when the flow in certain regions of the triple point structure becomes supersonic in the frame of reference of the triple point T or T'. Any Mach reflection requires $M_B^T > 1$; for $M_B^T < 1$ a regular reflection (RR) occurs. A single Mach reflection (SMR) pattern encompassing just the four states A to D is found for $M_C^T < 1$; for $M_C^T > 1$ a transitional or a double Mach reflection pattern occurs. In a DMR, the flow in C is also supersonic in the frame of reference of the secondary triple point T' ($M_C^{T'} > 1$), however, it is subsonic with $M_C^{T'} < 1$, in a TMR. Consequently, the secondary triple point T' is not fully developed in a TMR and the discontinuities R' and S' are absent. For given inflow velocity v_0 the transition points $M_{B/C}^T = 1$ are unique and can be determined rather easily by solving the corresponding set of oblique shock relations. The evaluation of the TMR/DMR transition point $M_C^{T'} = 1$ is more involved as knowledge of the velocity vector a of T' relative to T is required. The oblique shock relations between C and D readily yield $a_n \equiv 0$, however, the tangential velocity a_t of T' along R is a free parameter that needs to be specified separately.

Figure 5 visualizes the transition boundaries of the different shock wave reflection phenomena evaluated numerically for varying inflow Mach number. Since the estimation of the exact minimally possible value of a_t in a DMR is a considerable problem in itself, the TMR/DMR transition line is evaluated for the fixed value a_t = 100 m/s, which puts a reasonable upper transition boundary on the TMR region (dotted in Figure 5). Specially geared to detonations, results are displayed for the relative transverse wave strength S. We use the simulation results from Sections 3.1 and 3.3 as a first verification for the found quantitative transition boundaries. Throughout an unperturbed detonation cell only the DMR structure occurs, which is confirmed by plotting (with stars) beside the point at the end of a cell (cf. Figure 2) an additional one immediately after triple point collision. The open circles mark the triple point re-initiation visualized in the right graphic of Figure 3, and the transition boundaries clearly confirm the transition from TMR to DMR. The failing triple point shown in the right graphic of Figure 4 is marked with closed triangles indicating that the SMR pattern seems unstable for a detonation substructure and occurs only immediately before the triple point disappears.

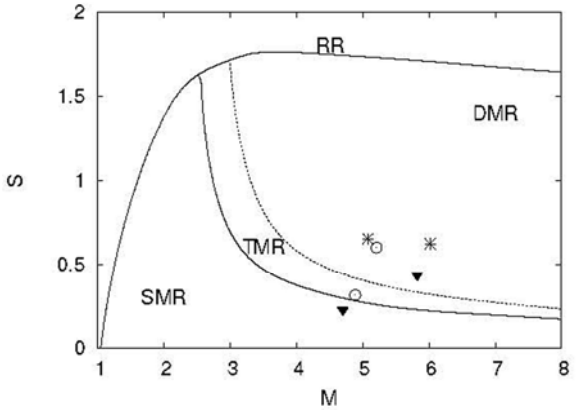

Figure 5. Transition boundaries of shock wave reflection phenomena for the nonreactive H2 : O2 : Ar mixture.

4. Conclusions

We have presented simulation results for gaseous detonations in two space dimensions in realistic geometry. The computations are fully resolved down to the scale of secondary triple points and can be used with confidence to analyze the evolving shock wave reflection structures. A crucial enabler for these simulations is the utilization of MPI-parallel dynamic structured adaptive mesh refinement which reduces the finest mesh size for the pipe bend studies by at least a factor of 250 and up to 680.

Nonreactive but thermally perfect shock wave reflection theory is used successfully to predict the transition boundaries between Mach reflection patterns depending on the inflow velocity. Exemplary transient triple points structures from the simulations are compared with the theoretical results and

good agreement in observed and predicted Mach reflection type is found. Future work will concentrate on deriving a physical estimate for the smallest possible relative tangential velocity a_t between primary and secondary triple point in a double Mach reflection to complete the theoretical model.

Acknowledgments
This work is sponsored by the Office of Advanced Scientific Computing Research; U.S. Department of Energy (DOE) and was performed at the Oak Ridge National Laboratory, which is managed by UT-Battelle, LLC under Contract No. DE-AC05-00OR22725.

References
[1] G. Ben-Dor. *Shock wave reflection phenomena*. Springer, Berlin, 2nd edition, 2007.
[2] M. Berger and P. Colella. Local adaptive mesh refinement for shock hydrodynamics. *J. Comput. Phys.*, 82:64–84, 1988.
[3] R. Deiterding. Construction and application of an AMR algorithm for distributed memory computers. In T. Plewa et, editors, *Adaptive Mesh Refinement—Theory and Applications*, volume 41 of *Lecture Notes in Computational Science and Engineering*, pages 361–372. Springer, 2005.
[4] R. Deiterding. Detonation structure simulation with AMROC. In L. T. Yang, editor, *High Performance Computing and Communications 2005*, volume 3726 of *Lecture Notes in Computer Science*, pages 916–927. Springer, 2005.
[5] R. Deiterding. A parallel adaptive method for simulating shock-induced combustion with detailed chemical kinetics in complex domains. *Computers & Structures*, 87:769–783, 2009.
[6] R. Deiterding and G. Bader. High-resolution simulation of detonations with detailed chemistry. In G. Warnecke, editor, *Analysis and Numerics for Conservation Laws*, pages 69–91. Springer, 2005.
[7] W. Fickett and W. C. Davis. *Detonation*. University of California Press, Berkeley and Los Angeles, California, 1979.
[8] X.Y. Hu, B.C. Khoo, D.L. Zhang, and Z.L. Jiang. The cellular structure of a two dimensional H_2/O_2/Ar detonation wave. *Combustion Theory & Modelling*, 8:339–359, 2004.
[9] R.A. Strehlow. Gas phase detonations: Recent developments. *Combust. Flame*, 12(2):81–101, 1968.
[10] C.K. Westbrook. Chemical kinetics of hydrocarbon oxidation in gaseous detonations. *Combust. Flame*, 46:191–210, 1982.